



The synthesis, crystal structure and Hirshfeld analysis of 4-(3,4-dimethylanilino)-*N*-(3,4-dimethylphenyl)quinoline-3-carboxamide

Ligia R. Gomes, John Nicolson Low, Fernanda Borges, Alexandra Gaspar and Francesco Mesiti

Acta Cryst. (2020). E76, 201–207



IUCr Journals

CRYSTALLOGRAPHY JOURNALS ONLINE

This open-access article is distributed under the terms of the Creative Commons Attribution Licence <http://creativecommons.org/licenses/by/4.0/legalcode>, which permits unrestricted use, distribution, and reproduction in any medium, provided the original authors and source are cited.





The synthesis, crystal structure and Hirshfeld analysis of 4-(3,4-dimethylanilino)-*N*-(3,4-dimethylphenyl)quinoline-3-carboxamide

Ligia R. Gomes,^{a,b} John Nicolson Low,^{c*} Fernanda Borges,^d Alexandra Gaspar^d and Francesco Mesiti^e

Received 1 January 2020

Accepted 10 January 2020

Edited by M. Zeller, Purdue University, USA

Keywords: crystal structure; hydrogen bonding; quinoline; carboxamide; amine.

CCDC reference: 1879928

Supporting information: this article has supporting information at journals.iucr.org/e

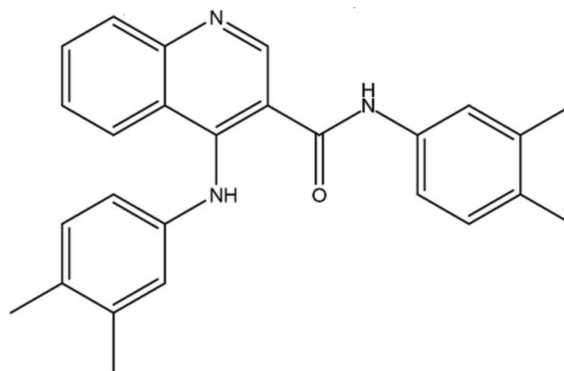
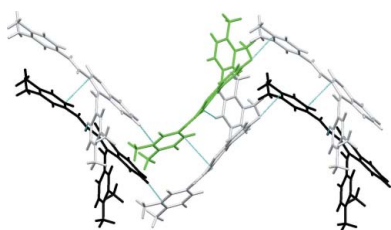
^aREQUIMTE, Departamento de Química e Bioquímica, Faculdade de Ciências da Universidade do Porto, Rua do Campo Alegre, 687, P-4169-007, Porto, Portugal, ^bFP-ENAS-Faculdade de Ciências de Saúde, Escola Superior de Saúde da UFP, Universidade Fernando Pessoa, Rua Carlos da Maia, 296, P-4200-150 Porto, Portugal, ^cDepartment of Chemistry, University of Aberdeen, Meston Walk, Old Aberdeen, AB24 3UE, Scotland, ^dCIQUP Departamento de Química e Bioquímica, Faculdade de Ciências, Universidade do Porto, 4169-007 Porto, Portugal, and ^eDepartment of "Scienze della Vita", University "Magna Graecia" of Catanzaro, Catanzaro, Italy. *Correspondence e-mail: jnlow111@gmail.com

The structure of the title quinoline carboxamide derivative, C₂₆H₂₅N₃O, is described. The quinoline moiety is not planar as a result of a slight puckering of the pyridine ring. The secondary amine has a slightly pyramidal geometry, certainly not planar. Both intra- and intermolecular hydrogen bonds are present. Hirshfeld surface analysis and lattice energies were used to investigate the intermolecular interactions.

1. Chemical context

Quinoline (1-aza-naphthalene or benzo[b]pyridine) is a natural heterocyclic building block often used as a template for derivatization and generation of drug-like libraries for the discovery of novel bioactive ligands (Mugnaini *et al.*, 2009; Musiol, 2017). Quinoline-based compounds are well known for their antimalarial activity (Antony & Parija, 2016), although a large spectrum of other biological activities, such as anticancer, antimicrobial, anti-inflammatory, antioxidant, antihypertensive and against neurodegenerative diseases, have also been ascribed to these types of heterocyclic compounds (Nainwal *et al.*, 2019).

This work is a continuation of our investigation into the preparation, structural analysis and pharmacological properties of substituted heterocyclics including, for example, new insights in the discovery of novel h-MAO-B inhibitors obtained by the structural characterization of a series of *N*-phenyl-4-oxo-4*H*-chromene-3-carboxamide derivatives (Gomes *et al.*, 2015*a*). Other chromone and coumarin carboxamides are discussed in Gomes *et al.* (2015*b*, 2016).



OPEN ACCESS

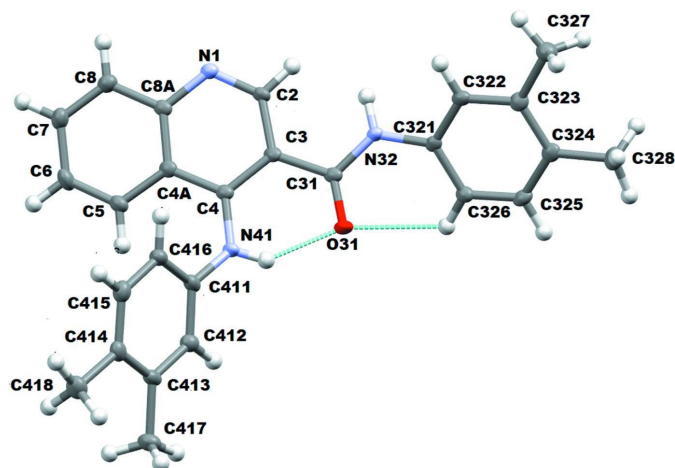


Figure 1
A view of the asymmetric unit of **1** with the atom-numbering scheme. Displacement ellipsoids are drawn at the 50% probability level.

Here we report the synthesis and structural characterization of a quinoline-3-carboxamide derivative, 4-(3,4-dimethylanilino)-*N*-(3,4-dimethylphenyl)quinoline-3-carboxamide, **1**.

2. Structural commentary

An ellipsoid plot for compound **1** is shown in Fig. 1. The quinoline ring system is not planar, with atoms C2 and C4 deviating from the mean plane of the quinoline ring by $-0.110(3)$ and $0.125(3)$ Å, respectively, and C6 lying $-0.100(3)$ Å below the mean plane. The pyridine ring is slightly puckered with a screw-boat conformation, $Q = 0.087(3)$ Å, $\theta = 106(2)^\circ$ and $\varphi = 25(2)^\circ$. The mean plane of this ring makes a dihedral angle of $7.49(13)^\circ$ with the mean plane of the benzene ring of the quinoline moiety. The angles between the mean planes of the quinoline ring and the benzene rings with pivot atoms C321 and C411 are $28.99(11)$ and $59.16(11)^\circ$ respectively. The dihedral angle between the mean plane of these benzene rings is $64.71(14)^\circ$.

The amide group attached to C3 is coplanar with the quinoline ring system. The C–N rotamer of the amide has an *anti* conformation placing the quinoline ring *trans* in relation to the ring with pivot atom C321. The amide group atoms are essentially coplanar with the quinoline ring with deviations of $-0.034(3)$, (C31), $-0.009(2)$ (O31), $0.009(2)$, (N32) and $0.145(3)$ Å (C321). The geometric arrangement of the amide permits the formation of an intramolecular hydrogen bond between the amine hydrogen atom and the carboxyl group of the amide, $N41-H41 \cdots O31$; geometric parameters are given in Table 1. A further intramolecular hydrogen bond, $C326-H326 \cdots O31$, occurs.

The secondary amine has a slightly pyramidal geometry, certainly not planar. The angles $C411-N41-C4$, $C41-N41-H41$ and $C411-N41-H41$ are $125.7(2)$, $112(2)$ and $115(2)^\circ$, respectively, the sum of which (352.7°) is less than 360° ; in addition, atom H41 lies $0.41(3)$ Å out of the C4/N41/C411 mean plane, confirming the sp^3 hybridization of N41. An inspection of the amine bond lengths shows that there is a

Table 1
Hydrogen-bond geometry (Å, $^\circ$).

C_g is the centroid of the N1/C2–C4/C4A/C8A ring.

<i>D</i> –H \cdots <i>A</i>	<i>D</i> –H	H \cdots <i>A</i>	<i>D</i> \cdots <i>A</i>	<i>D</i> –H \cdots <i>A</i>
N41–H41 \cdots O31	0.84(4)	1.93(3)	2.635(3)	142(3)
C326–H326 \cdots O31	0.95	2.40	2.887(3)	112
N32–H32 \cdots N1 ⁱ	0.90(4)	2.07(4)	2.891(3)	150(3)
C2–H2 \cdots N1 ⁱ	0.96(3)	2.55(3)	3.477(4)	163(2)
C416–H416 \cdots O31 ⁱⁱ	0.95	2.39	3.252(4)	150
C326–H326 \cdots C _g ⁱⁱⁱ	0.95	2.82	3.398(3)	120

Symmetry codes: (i) $x + \frac{1}{2}, -y + \frac{3}{2}, -z + 1$; (ii) $x - 1, y, z$; (iii) $x + 1, y, z$.

slight asymmetry of the electronic distribution around it: C4–N41 = $1.364(3)$ Å while N41–C411 = $1.437(4)$ Å, suggesting there is higher density between the nitrogen and the carbon atom of the quinoline ring system. However, these bonds and angles are typical for a $C_{\text{quinoline}}\text{-NH-C-R}$ group, see the *Database Survey* below. As a consequence of the screw-boat pucker of the pyridine ring, the C4–N41 bond is displaced from the pyridine mean plane with a deviation of $0.159(2)$ Å for N41; atom C411 is displaced by $0.965(3)$ Å and consequently, the N41–C411 bond lies further from the mean plane.

3. Supramolecular features

In the crystal, the molecules are linked by $N32-H32 \cdots N1(x + \frac{1}{2}, -y + \frac{3}{2}, -z + 1)$, hydrogen bonds, forming C_6 chains which run parallel to the *a*-axis formed by the action of the 2_1 screw axis at $(\frac{1}{2}, 0, \frac{3}{4})$. This is supplemented by the weak $C2-H2 \cdots N1(x + \frac{1}{2}, -y + \frac{3}{2}, -z + 1)$ hydrogen bond, Table 1 and Fig. 2. The other weak hydrogen bonds, C416–

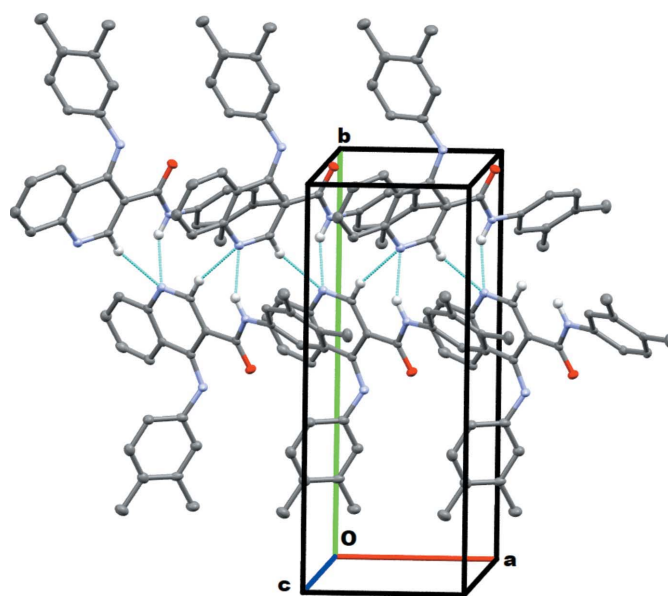
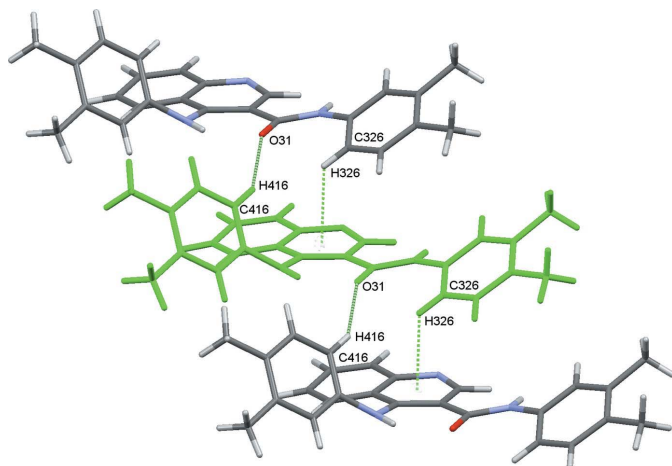


Figure 2
A view of the $N32-H32 \cdots N1$ C_6 chain running along the *a* axis with the supplementary $C2-H2 \cdots N1$ bond. Hydrogen atoms not involved in the hydrogen bonding are omitted for clarity.


Figure 3

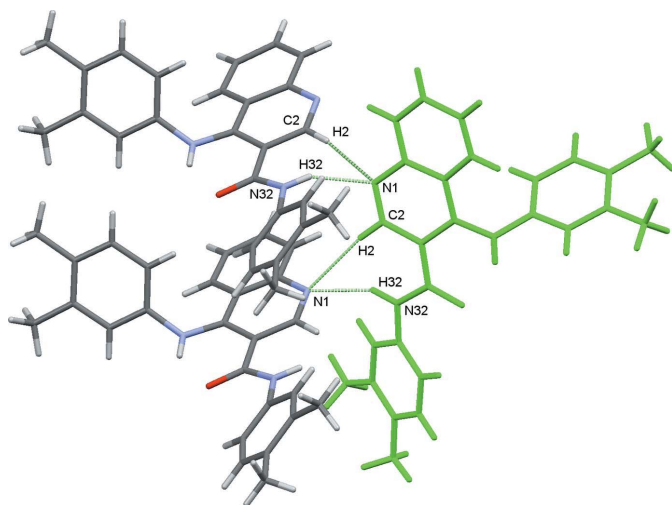
Molecule pairs **Ia/Ib**: $x - 1, y, z$ (top) and $x + 1, y, z$ (bottom). Values of energies by pair: $E_{\text{tot}} = -55.9 \text{ kJ mol}^{-1}$, $E_{\text{coul}} = -21.4 \text{ kJ mol}^{-1}$, $E_{\text{pol}} = -10.0 \text{ kJ mol}^{-1}$, $E_{\text{disp}} = -79.5 \text{ kJ mol}^{-1}$ and $E_{\text{rep}} = 55.0 \text{ kJ mol}^{-1}$. Interaction energies were calculated using *PIXEL3.1* (Gavezzotti, 2003, 2008) based on densities computed with G09 using the mp2/6-31** level of theory.

H416...O31 and C418—H41B...O31, both involve atom O31 as an acceptor and link the chains described above to form a sheet which extends along the b -axis direction.

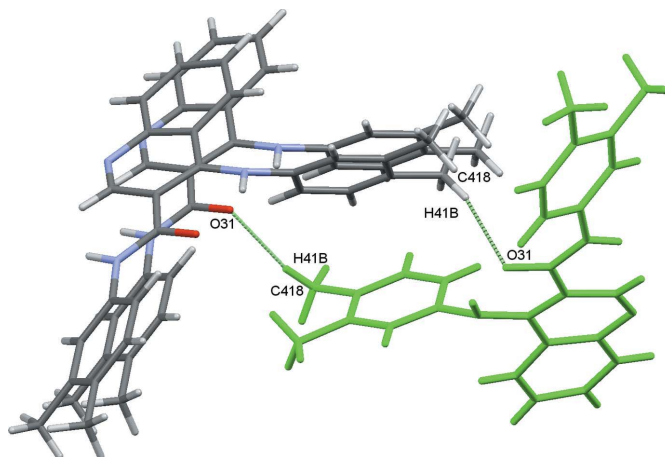
No π - π interactions occur but there is a possible C—H... π interaction, C326—H326...Cg, involving the pyridine ring (Table 1), which is discussed more fully below.

4. Hirshfeld surface analysis and lattice energies

Hirshfeld surfaces (McKinnon *et al.*, 2004) and two-dimensional fingerprint (FP) plots provide complementary information concerning the intermolecular interactions discussed

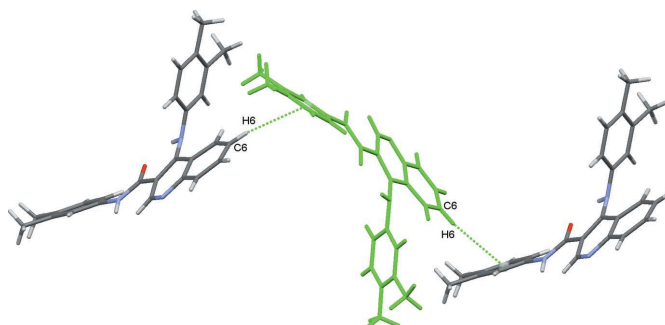

Figure 4

Molecule pairs **IIa/IIb**: $x - \frac{1}{2}, -y + \frac{3}{2}, -z + 1$ (top) and $x - \frac{1}{2}, -y + \frac{3}{2}, -z + \frac{1}{2}$ (bottom). Values of energies by pair: $E_{\text{tot}} = -52.3 \text{ kJ mol}^{-1}$, $E_{\text{coul}} = -59.10 \text{ kJ mol}^{-1}$, $E_{\text{pol}} = -26.9 \text{ kJ mol}^{-1}$, $E_{\text{disp}} = -41.5 \text{ kJ mol}^{-1}$ and $E_{\text{rep}} = 75.2 \text{ kJ mol}^{-1}$. Interaction energies were calculated using *PIXEL3.1* (Gavezzotti, 2003, 2008) based on densities computed with G09 using the mp2/6-31** level of theory.


Figure 5

Molecule pairs **IIIa/IIIb**: $(x + \frac{1}{2}, -y + \frac{1}{2}, z + 1)$ (top) and $(x - \frac{1}{2}, -y + \frac{1}{2}, z + 1)$ (bottom). Values of energies by pair: $E_{\text{tot}} = -30.0 \text{ kJ mol}^{-1}$, $E_{\text{coul}} = -11.3 \text{ kJ mol}^{-1}$, $E_{\text{pol}} = -4.5 \text{ kJ mol}^{-1}$, $E_{\text{disp}} = -36.0 \text{ kJ mol}^{-1}$, $E_{\text{rep}} = 21.8 \text{ kJ mol}^{-1}$. Interaction energies were calculated using *PIXEL3.1* (Gavezzotti, 2003, 2008) based on densities computed with G09 using the mp2/6-31** level of theory.

above. The analyses were generated using *Crystal Explorer 3.1* (Wolff *et al.*, 2012). The lattice energies for **1** were analysed after performing calculations as implemented in the *PIXEL* program (Gavezzotti, 2003, 2008). The total stabilization energy of the crystal packing, E_{tot} is $-207.0 \text{ kJ mol}^{-1}$, distributed as Coulombic, ($E_{\text{coul}} = -112.9 \text{ kJ mol}^{-1}$), polarization ($E_{\text{pol}} = -52.8 \text{ kJ mol}^{-1}$), dispersion ($E_{\text{disp}} = -251.6 \text{ kJ mol}^{-1}$) and repulsion ($E_{\text{rep}} = 210.4 \text{ kJ mol}^{-1}$). The dispersive energy contributes the most to the total stabilization energy of the lattice, in addition to the C—H...O hydrogen bonds, and to the C—H... π interaction. The stabilization energy comes from six sub-structural motifs made by the molecule pairs **I** to **VI** that are shown in Figs. 3 to 8, together with the symmetry codes as well as the respective energies. They contribute a total energy of $-369.4 \text{ kJ mol}^{-1}$ for the lattice, half of it, $-184.7 \text{ kJ mol}^{-1}$ attributed to the (x, y, z) molecule. That energy corresponds approximately to 88% of the total stabilization energy of the network.


Figure 6

Molecule pairs **IVa/IVb**: $-x + \frac{1}{2}, -y + 1, z + \frac{1}{2}$ (left) and $-x + \frac{1}{2}, -y + 1, z - \frac{1}{2}$ (right). Values of energies by pair: $E_{\text{tot}} = -20.7 \text{ kJ mol}^{-1}$, $E_{\text{coul}} = -7.4 \text{ kJ mol}^{-1}$, $E_{\text{pol}} = -4.4 \text{ kJ mol}^{-1}$, $E_{\text{disp}} = -31.3 \text{ kJ mol}^{-1}$, $E_{\text{rep}} = 22.5 \text{ kJ mol}^{-1}$. Interaction energies were calculated using *PIXEL3.1* (Gavezzotti, 2003, 2008) based on densities computed with G09 using the mp2/6-31** level of theory.

Table 2
Percentages for atom...atom close contacts.

Compound	H...H	H...O/O...H	H...C/C...H	C...C	O...C/C...O	N...N	H...N/N...H	C...N/N...C
1	58.4	4.3	27.0	2.5	0.6	0.2	6.5	0.5

The percentages of atom...atom close contacts taken from the FP plot (McKinnon *et al.*, 2004) for **1** shows that, apart from the H...H contacts (58.4%), there are high percentages of C...H/H...C close contacts (27.0%) and of N...H/H...N close contacts (6.5%), see Table 2.

Apart from the intramolecular hydrogen bond with N41, the carboxyl oxygen atom O31 involves its lone pairs in another two intermolecular C—H...O interactions, O31...H416—C416 and O31...H41B—C418. The first inter-

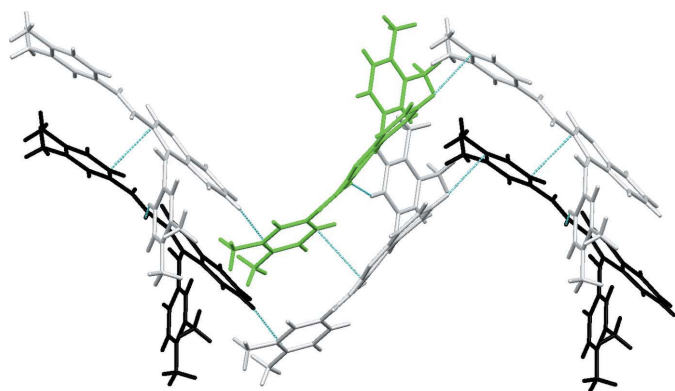


Figure 7
Molecule pairs **Va/Vb**: $-x + \frac{3}{2}, y + 1, z - \frac{1}{2}$ (left) and $-x + \frac{3}{2}, y + 1, z + \frac{1}{2}$ (right). Values of energies by pair: $E_{\text{tot}} = -14.5 \text{ kJ mol}^{-1}$, $E_{\text{coul}} = -5.0 \text{ kJ mol}^{-1}$, $E_{\text{pol}} = -2.5 \text{ kJ mol}^{-1}$, $E_{\text{disp}} = -23.4 \text{ kJ mol}^{-1}$, $E_{\text{rep}} = 16.4 \text{ kJ mol}^{-1}$. Interaction energies were calculated using *PIXEL3.1* (Gavezzotti, 2003, 2008) based on densities computed with G09 using the mp2/6-31** level of theory.

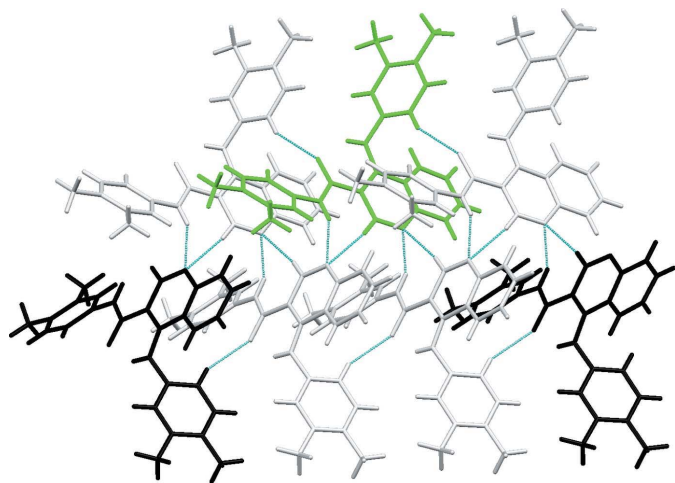


Figure 8
Molecule pairs **VIa/VIb**, $(x - \frac{3}{2}, -y + \frac{3}{2}, -z + 1)$ (left) and $(x - \frac{3}{2}, -y + \frac{3}{2}, -z + 1)$ (right). Values of energies by pair: $E_{\text{tot}} = -11.3 \text{ kJ mol}^{-1}$, $E_{\text{coul}} = -3.3 \text{ kJ mol}^{-1}$, $E_{\text{pol}} = -2.2 \text{ kJ mol}^{-1}$, $E_{\text{disp}} = -15.5 \text{ kJ mol}^{-1}$, $E_{\text{rep}} = 9.6 \text{ kJ mol}^{-1}$. Interaction energies were calculated using *PIXEL3.1* (Gavezzotti, 2003, 2008) based on densities computed with G09 using the mp2/6-31** level of theory.

action creates chains running along the *a*-axis direction that are further stabilized by C—H... π interactions (C326—H326...C_g_{pyridine}), as can be identified by the red spots in the Hirshfeld Surface (McKinnon *et al.*, 2004) for the molecule, Fig. 9, and they form two molecule pairs, identified as substructures **Ia/Ib** in Fig. 3. Each of those pairs contribute $-55.9 \text{ kJ mol}^{-1}$ to the stabilization of the lattice, mainly dispersion energy. The second interaction, O31...H41B—C418, makes another two molecule pairs, **IIIa/IIIb**, Fig. 5. In this substructure the Coulombic energy is higher than the dispersive energy, which is indicative of the minor importance of the interactions involving the aromatic rings. These hydrogen bonds can also be identified as red spots in the HS, Fig. 9.

The nitrogen atom N32 acts as a donor for N1 (N32—H32...N1). N1 also acts as an acceptor for C6, making a C6—H6...N1 hydrogen bond, seen as a red spot in Fig. 9. Those interactions give sub structural motifs **IIa/IIb**, Fig. 4. The molecules are linked by N32—H32...N1($x + \frac{1}{2}, -y + \frac{3}{2}, -z + 1$) hydrogen bonds, forming C6 chains which run parallel to the *a*-axis direction, formed by the action of the 2_1 screw axis at $(\frac{1}{2}, 0, \frac{3}{4})$. This is supplemented by the weak C2—H2...N1($x + \frac{1}{2}, -y + \frac{3}{2}, -z + 1$) hydrogen bond, Figs. 3 and 4.

In addition, the C—H... π interaction can also be identified in the HS of the molecule, Fig. 9. The interaction connects the molecules in zigzag chains running along the *c*-axis direction, as a result of the propagation of the molecule pairs **IVa/IVb** depicted in Fig. 6.

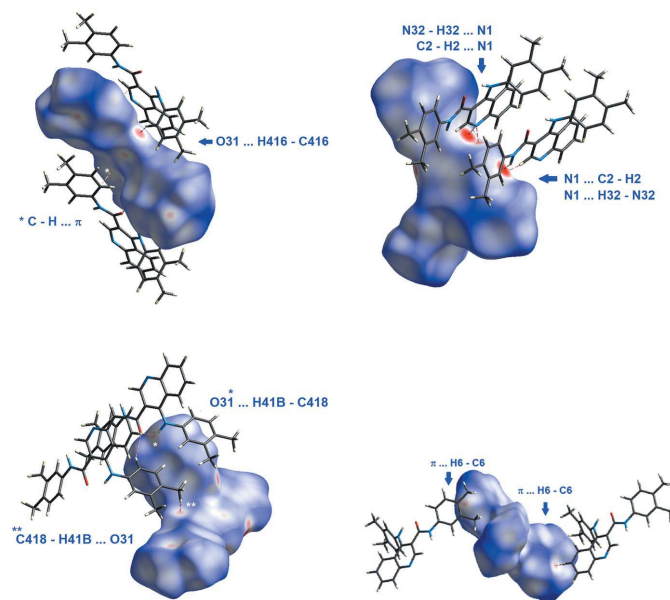


Figure 9
Several faces of the HS plotted over d_{norm} for **1** showing the red spots that indicate close contacts between atoms, which are identified in the figures.

Apart from the sub-structural motifs described, there are two extra molecule pairs, identified as **Va/Vb** and **Vla/VIb**, which are also illustrated in Figs. 7 and 8: the two molecules involved are at x, y, z (green-coloured molecule) and $-x + \frac{3}{2}, -y + 1, z - \frac{1}{2} - x + \frac{3}{2}, -y + 1, z + \frac{1}{2}$ (black-coloured molecule) for **Va/Vb** and $x - \frac{3}{2}, -y + \frac{3}{2}, -z + 1/x - \frac{3}{2}, -y + \frac{3}{2}, -z + 1$ for **Vla/VIb**. Although these molecules do not exhibit atom...atom close contacts, each pair provides a significant contribution to the overall lattice stabilization energy of -14.5 and -11.3 kJ mol $^{-1}$, respectively for **V** and **VI**. The grey molecules drawn in this figure indicate a possible pathway for electronic delocalization within the network of molecules.

5. Database survey

A search of the Cambridge Structural Database (CSD, Version 5.40, November 2019 update; Groom *et al.*, 2016) for 3,4-disubstituted quinoline with an N–H unit attached to C4 revealed two compounds: SEZJIR (3-acetyl-4-aminoquinoline; Lokaj *et al.*, 2007) with a carbonyl group attached to C3 and an amino group attached to C4 and PABPUD [4-[3-(*N,N*-dimethylamino)propylamino]-3-nitroquinoline; Boyd *et al.*, 1992] with an amino group attached to C4 and a nitro group attached to C3. In both of these compounds, there is no puckering of the pyridine ring and the quinoline ring system is essentially planar. In both cases, a hydrogen atom forms an intramolecular hydrogen bond between an amino hydrogen and the carbonyl oxygen in both independent molecules of the asymmetric unit (SEZJIR) or between the amino hydrogen and a nitro group oxygen atom (PABPUD). In both structures, the C(pyridine)...N(amino) distances are significantly shorter than those in **1**, *viz.* 1.325 and 1.335 Å for the two molecules in the asymmetric unit of SEZJIR and 1.320 Å in PABPUD. The corresponding value in **1** is 1.364 (3) Å.

A survey of quinoline compounds, with an *R* factor of 10% or less with a C_{quinoline}–NH–C_{aryl/sp³} unit attached to C4 of the quinoline moiety gave 56 hits for 63 individual molecules, including **1**. The C_{quinoline}–N distances lie in the range 1.319 to 1.438 Å with an average value of 1.360 Å.

The situation is more complex for the N–C_{aryl/sp³} bond and for the C_{quinoline}–N–C_{aryl/sp³} angle. A scatterplot of these revealed two populations, one in which the N atom is attached to a benzene ring and the other in which the connection is to an *sp*³ carbon. UNIKUZ [6-(*t*-butylsulfonyl)-*N*-(5-fluoro-1*H*-indazol-3-yl)quinolin-4-amine methanol solvate; Haile *et al.*, 2016] is included in the first group. The C_{aryl}–N distances lie in the range 1.396 to 1.438 Å with an average value of 1.418 Å and an average C_{quinoline}–N–C_{aryl/sp³} angle of 126.105°. In the second case, the C_{aryl/sp³}–N distances lie in the range 1.439 to 1.478 Å with an average value of 1.458 Å, with an average C_{quinoline}–N–C_{aryl/sp³} angle of 123.98°.

As noted above, the conformation around the amino N atom is slightly pyramidal. In their paper on bond lengths in organic compounds, Allen *et al.* (2006) discuss the planarity and pyramidalicity of amino compounds. They state that for planar N atoms, the mean valence angle is greater than 117.6°

while for pyramidal N atoms the mean valence angle lies in the range 108 to 114°. The value for **1** is 117.56°. There are three other structures in this survey which have average valence angles close to but less than 117°. The valence angles are 116.57° in DAMIOT [2,3-bis[(2,6-dimethylphenyl)sulfanyl]-*N*-phenylquinolin-4-amine; Florke & Egold, 2016], 117.41° in MEQKEY (2,4-dianilino-3-ethylquinoline; Katritzky *et al.*, 2000) and 117.04° in OTAMOM [2-(4-methoxyphenyl)-*N*-(2-(2-phenylvinyl)phenyl)quinolin-4-amine; Mphahlele & Mphahlele, 2011]. These four compounds are thus neither strictly planar nor pyramidal.

There are two compounds in the database which have an amide group attached to C3, GICGIL [2-chloro-*N*-(4-fluorophenyl)-6-methylquinoline-3-carboxamide; Govender *et al.*, 2018] and SUZHEB (*N*-isopropyl-6-methyl-2-phenylquinoline-3-carboxamide; Benzerka *et al.*, 2010). In both these compounds, the amide group is inclined to the quinoline moiety, unlike in molecule **1**.

6. Synthesis and crystallization

The title quinolone derivative **1** was synthesized by a one-pot reaction between 4-oxo-1,4-dihydroquinoline-3-carboxylic acid and 3,4-dimethylaniline in the presence of POCl₃ following a procedure described previously (Cagide *et al.*, 2015). The title compound was obtained in 70% yield and characterized by NMR. It was re-crystallized from dichloromethane to yield crystals suitable for X-ray diffraction, m.p. 489–493 K.

NMR data were acquired on a Bruker AMX 400 spectrometer, recorded at room temperature in 5 mm outer-diameter tubes. The samples were prepared in deuterated dimethylsulfoxide (DMSO) with tetramethylsilane (TMS) as internal reference. Chemical shifts are expressed as δ (ppm) values relative to TMS; coupling constants (*J*) are given in Hz. Atoms are labelled with their numerical designation as per Fig. 1. See *Supporting Information* for spectra.

4-(3,4-Dimethylanilino)-*N*-(3,4-dimethylphenyl)quinoline-3-carboxamide

¹H NMR (400 MHz, DMSO): 10.16 (1H, *s*, CONH), 9.43 (1H, *s*, NH), 8.82 (1H, *s*, H-2), 8.14 (1H, *dd*, *J* = 1.0, 8.5 Hz, H-8), 7.95 (1H, *dd*, *J* = 0.84, 8.4 Hz, H-5), 7.73 (1H, *ddd*, *J* = 1.0, 6.9, 8.4 Hz, H-6), 7.46 (1H, *ddd*, *J* = 1.0, 6.9, 8.5 Hz, H-7), 7.18 (1H, *d*, *J* = 2.0 Hz, H-412), 7.12 (1H, *dd*, *J* = 2.1, 8.0 Hz, H-326), 7.00 (1H, *d*, *J* = 8.0 Hz, H-325), 6.93 (1H, *d*, *J* = 8.0 Hz, H-415), 6.84 (1H, *d*, *J* = 2.1 Hz, H-322), 6.72 (1H, *dd*, *J* = 2.0, 8.0 Hz, H-416), 2.01 (3H, *s*, CH₃), 2.07 (3H, *s*, CH₃), 2.16 (6H, *s*, 2 × CH₃).

¹³C NMR (100 MHz, DMSO): 165.4 (CONH), 149.9 (C-2), 149.1 (C-8A), 146.6 (C-4), 140.3 (C-411), 136.5 (C-414), 136.3 (C-321), 135.6 (C-324), 131.2 (C-413), 130.5 (C-323), 130.2 (C-6), 129.6 (C-415), 129.2 (C-5), 129.0 (C-325), 125.0 (C-7), 124.2 (C-8), 121.6 (C-412), 121.5 (C-322), 120.8 (C-4A), 117.8 (C-325), 117.7 (C-416), 114.4 (C-3), 19.5 (CH₃), 19.3 (CH₃), 18.7 (CH₃), 18.5 (CH₃).

7. Refinement

Crystal data, data collection and structure refinement details are summarized in Table 3. The H atoms were included in idealized positions and treated as riding atoms: C–H = 0.95–0.98 Å with $U_{\text{iso}}(\text{H}) = 1.2U_{\text{eq}}(\text{C})$ or $1.5U_{\text{eq}}(\text{C})$ for methyl H atoms. Those attached to N and C2 [C–H = 0.96 (3) Å] were refined. The latter was refined since it is involved in a short contact with H32, which is attached to N32. Although in the riding model for H2 the H-atom position is within the highest contour on the difference map, it is not at the centre. In the refined model it is. The H...H distances are 1.87 and 1.93 Å for the riding and refined models, respectively. The angles around C2 are N1–C2–C3 = 125.9 (3) and 125.9°(3); N–C2–H2 = 117 and 111.9 (17)° and C3–C2–H2 = 117 and 122.2 (17)° for riding and refined H atoms, respectively. In the case of H32, the N32–H32 distance changes from 0.89 (3) to 0.90 (4) Å and the angle C31–N32–H32 changes from 120 (2) to 119 (2)° for riding to refined, respectively, which are really insignificant shifts. Hence, in this case the short contact does induce a shift in the angular position of H2 from its calculated position.

Acknowledgements

The authors thank the staff at the National Crystallographic Service, University of Southampton, for the data collection, help and advice (Coles & Gale, 2012).

Funding information

This work was funded by FEDER funds through the Operational Programme Competitiveness Factors – COMPETE – and national funds by the FCT – Foundation for Science and Technology –under research grants UID/QUI/00081 and PTDC/ASP-PES/28397/2017.

References

- Allen, F. R., Watson, D. G., Brammer, L., Orpen, A. G. & Taylor, R. (2006). *International Tables for Crystallography*, Vol. C, ch. 9.5, pp. 790–811. Chester: IUCr
- Antony, H. A. & Parija, S. C. (2016). *Trop. Parasitol.* **6**, 30–41.
- Benzerka, S., Bouraiou, A., Bouacida, S., Roisnel, T. & Belfaitah, A. (2010). *Acta Cryst.* **E66**, o2304–o2305.
- Boyd, M., Boyd, P. D. W., Atwell, G. J., Wilson, W. R. & Denny, W. A. (1992). *J. Chem. Soc. Perkin Trans. 2*, pp. 579–585.
- Cagide, F., Silva, T., Reis, J., Gaspar, A., Borges, F., Gomes, L. R. & Low, J. N. (2015). *Chem. Commun.* **51**, 2832–2835.
- Coles, S. J. & Gale, P. A. (2012). *Chem. Sci.* **3**, 683–689.
- Florke, U. & Egold, H. (2016). Private Communication (refcode DAMIOT). CCDC, Cambridge, England.
- Gavezzotti, A. (2003). *J. Phys. Chem. B*, **107**, 2344–2353.
- Gavezzotti, A. (2008). *Mol. Phys.* **106**, 1473–1485.
- Gomes, L. R., Low, J. N., Cagide, F., Chavarria, D. & Borges, F. (2015a). *Acta Cryst.* **E71**, 547–554.
- Gomes, L. R., Low, J. N., Cagide, F., Gaspar, A. & Borges, F. (2015b). *Acta Cryst.* **E71**, 1270–1277.
- Gomes, L. R., Low, J. N., Fonseca, A., Matos, M. J. & Borges, F. (2016). *Acta Cryst.* **E72**, 926–932.
- Govender, H., Mocktar, C. & Koorbanally, N. A. (2018). *J. Heterocycl. Chem.* **55**, 1002–1009.

Table 3

Experimental details.

Crystal data	
Chemical formula	C ₂₆ H ₂₅ N ₃ O
M_r	395.49
Crystal system, space group	Orthorhombic, $P2_12_12_1$
Temperature (K)	100
a, b, c (Å)	6.2502 (3), 15.7915 (6), 20.7395 (9)
V (Å ³)	2046.99 (15)
Z	4
Radiation type	Mo $K\alpha$
μ (mm ⁻¹)	0.08
Crystal size (mm)	0.30 × 0.05 × 0.01
Data collection	
Diffractometer	Rigaku FRE+ equipped with VHF Varimax confocal mirrors and an AFC12 goniometer and HyPix 6000 detector
Absorption correction	Multi-scan (<i>CrysAlis PRO</i> ; Rigaku OD, 2018)
$T_{\text{min}}, T_{\text{max}}$	0.487, 1.000
No. of measured, independent and observed [$I > 2\sigma(I)$] reflections	28997, 3754, 3390
R_{int}	0.089
($\sin \theta/\lambda$) _{max} (Å ⁻¹)	0.602
Refinement	
$R[F^2 > 2\sigma(F^2)], wR(F^2), S$	0.044, 0.094, 1.08
No. of reflections	3754
No. of parameters	287
H-atom treatment	H atoms treated by a mixture of independent and constrained refinement
$\Delta\rho_{\text{max}}, \Delta\rho_{\text{min}}$ (e Å ⁻³)	0.22, -0.20
Absolute structure	Flack x determined using 1238 quotients $[(I^-)-(I^+)]/[(I^-)+(I^+)]$ (Parsons <i>et al.</i> , 2013)
Absolute structure parameter	0.2 (10)

Computer programs: *CrysAlis PRO* (Rigaku OD, 2018), *SHELXT* (Sheldrick, 2015a), *ShelXle* (Hübschle *et al.*, 2011), *SHELXL20147* (Sheldrick, 2015b), *OSCAIL* (McArdle *et al.*, 2004), *Mercury* (Macrae *et al.*, 2006) and *PLATON* (Spek, 2020).

- Groom, C. R., Bruno, I. J., Lightfoot, M. P. & Ward, S. C. (2016). *Acta Cryst.* **B72**, 171–179.
- Haile, P. A., Votta, B. J., Marquis, R. W., Bury, M. J., Mehlmann, J. F., Singhaus, R. Jr, Charnley, A. K., Lakdawala, A. S., Convery, M. A., Lipshutz, D. B., Desai, B. M., Swift, B., Capriotti, C. A., Berger, S. B., Majahan, M. K., Reilly, M. A., Rivera, E. J., Sun, H. H., Nagilla, R., Beal, A. M., Finger, J. N., Cook, M. N., King, B. W., Ouellette, M. T., Totoritis, R. D., Pierdomenico, M., Negroni, A., Stronati, L., Cucchiara, S., Ziolkowski, B., Vossenkamper, A., MacDonald, T. T., Gough, P. J., Bertin, J. & Casillas, L. N. (2016). *J. Med. Chem.* **59**, 4876–4880.
- Hübschle, C. B., Sheldrick, G. M. & Dittrich, B. (2011). *J. Appl. Cryst.* **44**, 1281–1284.
- Katritzky, A. R., Huang, T.-B., Voronkov, M. V. & Steel, P. J. (2000). *J. Org. Chem.* **65**, 8069–8073.
- Lokaj, J., Kettmann, V., Černuchová, P., Milata, V. & Fronc, M. (2007). *Acta Cryst.* **E63**, o1164–o1166.
- Macrae, C. F., Edgington, P. R., McCabe, P., Pidcock, E., Shields, G. P., Taylor, R., Towler, M. & van de Streek, J. (2006). *J. Appl. Cryst.* **39**, 453–457.
- McArdle, P., Gilligan, K., Cunningham, D., Dark, R. & Mahon, M. (2004). *CrystEngComm*, **6**, 303–309.
- McKinnon, J. J., Spackman, M. A. & Mitchell, A. S. (2004). *Acta Cryst.* **B60**, 627–668.
- Mphahlele, M. J. & Mphahlele, M. M. (2011). *Tetrahedron*, **67**, 4689–4695.

- Mugnaini, C., Pasquini, S. & Corelli, F. (2009). *Curr. Med. Chem.* **16**, 1746–1767.
- Musiol, R. (2017). *Exp. Opin. Drug. Discov.* **12**, 583–597.
- Nainwal, L. M., Tasneem, S., Akhtar, W., Verma, G., Khan, M. F., Parvez, S., Shaquiquzaman, M., Akhter, M. & Alam, M. M. (2019). *Eur. J. Med. Chem.* **164**, 121–170.
- Parsons, S., Flack, H. D. & Wagner, T. (2013). *Acta Cryst.* **B69**, 249–259.
- Rigaku OD (2018). *CrysAlis PRO*. Rigaku Corporation, Tokyo, Japan.
- Sheldrick, G. M. (2015a). *Acta Cryst.* **A71**, 3–8.
- Sheldrick, G. M. (2015b). *Acta Cryst.* **C71**, 3–8.
- Spek, A. L. (2020). *Acta Cryst.* **E76**, 1–11.
- Wolff, S. K., Grimwood, D. I., McKinnon, J. J., Turner, M. J., Jayatilaka, D. & Spackman, M. A. (2012). *Crystal Explorer*. The University of Western Australia.

supporting information

Acta Cryst. (2020). E76, 201-207 [https://doi.org/10.1107/S2056989020000298]

The synthesis, crystal structure and Hirshfeld analysis of 4-(3,4-dimethylanilino)-*N*-(3,4-dimethylphenyl)quinoline-3-carboxamide

Ligia R. Gomes, John Nicolson Low, Fernanda Borges, Alexandra Gaspar and Francesco Mesiti

Computing details

Data collection: *CrysAlis PRO* (Rigaku OD, 2018); cell refinement: *CrysAlis PRO* (Rigaku OD, 2018); data reduction: *CrysAlis PRO* (Rigaku OD, 2018); program(s) used to solve structure: *OSCAIL* (McArdle *et al.*, 2004) and *SHELXT* (Sheldrick, 2015a); program(s) used to refine structure: *OSCAIL* (McArdle *et al.*, 2004), *ShelXle* (Hübschle *et al.*, 2011) and *SHELXL2014/7* (Sheldrick, 2015b); molecular graphics: *Mercury* (Macrae *et al.*, 2006); software used to prepare material for publication: *OSCAIL* (McArdle *et al.*, 2004), *SHELXL2014* (Sheldrick, 2015b) and *PLATON* (Spek, 2020).

4-(3,4-Dimethylanilino)-*N*-(3,4-dimethylphenyl)quinoline-3-carboxamide

Crystal data

$C_{26}H_{25}N_3O$

$M_r = 395.49$

Orthorhombic, $P2_12_12_1$

$a = 6.2502$ (3) Å

$b = 15.7915$ (6) Å

$c = 20.7395$ (9) Å

$V = 2046.99$ (15) Å³

$Z = 4$

$F(000) = 840$

$D_x = 1.283$ Mg m⁻³

Mo $K\alpha$ radiation, $\lambda = 0.71075$ Å

Cell parameters from 5133 reflections

$\theta = 1.6$ – 27.0°

$\mu = 0.08$ mm⁻¹

$T = 100$ K

Needle, yellow

$0.30 \times 0.05 \times 0.01$ mm

Data collection

Rigaku FRE+ equipped with VHF Varimax confocal mirrors and an AFC12 goniometer and HyPix 6000 detector diffractometer

Radiation source: Rotating Anode, Rigaku FRE+

Confocal mirrors, VHF Varimax monochromator

Detector resolution: 10 pixels mm⁻¹ profile data from ω -scans

Absorption correction: multi-scan (*CrysAlis PRO*; Rigaku OD, 2018)

$T_{\min} = 0.487$, $T_{\max} = 1.000$

28997 measured reflections

3754 independent reflections

3390 reflections with $I > 2\sigma(I)$

$R_{\text{int}} = 0.089$

$\theta_{\max} = 25.4^\circ$, $\theta_{\min} = 1.6^\circ$

$h = -7 \rightarrow 7$

$k = -19 \rightarrow 19$

$l = -24 \rightarrow 24$

Refinement

Refinement on F^2

Least-squares matrix: full

$R[F^2 > 2\sigma(F^2)] = 0.044$

$wR(F^2) = 0.094$

$S = 1.08$

3754 reflections

287 parameters

0 restraints

Primary atom site location: structure-invariant direct methods

Secondary atom site location: structure-invariant direct methods

Hydrogen site location: mixed
 H atoms treated by a mixture of independent
 and constrained refinement
 $w = 1/[\sigma^2(F_o^2) + (0.0402P)^2 + 0.5091P]$
 where $P = (F_o^2 + 2F_c^2)/3$
 $(\Delta/\sigma)_{\max} < 0.001$

$\Delta\rho_{\max} = 0.22 \text{ e } \text{\AA}^{-3}$
 $\Delta\rho_{\min} = -0.20 \text{ e } \text{\AA}^{-3}$
 Absolute structure: Flack x determined using
 1238 quotients $[(I^+)-(I^-)]/[(I^+)+(I^-)]$ (Parsons *et al.*, 2013)
 Absolute structure parameter: 0.2 (10)

Special details

Geometry. All esds (except the esd in the dihedral angle between two l.s. planes) are estimated using the full covariance matrix. The cell esds are taken into account individually in the estimation of esds in distances, angles and torsion angles; correlations between esds in cell parameters are only used when they are defined by crystal symmetry. An approximate (isotropic) treatment of cell esds is used for estimating esds involving l.s. planes.

Fractional atomic coordinates and isotropic or equivalent isotropic displacement parameters (\AA^2)

	<i>x</i>	<i>y</i>	<i>z</i>	$U_{\text{iso}}^*/U_{\text{eq}}$
O31	0.5597 (3)	0.49964 (12)	0.49759 (10)	0.0221 (5)
N1	-0.0092 (4)	0.69133 (14)	0.44267 (11)	0.0174 (5)
N32	0.5344 (4)	0.62696 (15)	0.54659 (11)	0.0162 (5)
H32	0.470 (5)	0.678 (2)	0.5477 (15)	0.028 (9)*
N41	0.2497 (4)	0.44714 (15)	0.42129 (13)	0.0195 (5)
H41	0.368 (6)	0.441 (2)	0.4400 (16)	0.026 (9)*
C2	0.1722 (5)	0.66921 (17)	0.47005 (13)	0.0161 (6)
H2	0.233 (5)	0.7147 (17)	0.4948 (14)	0.014 (7)*
C3	0.2727 (4)	0.58912 (17)	0.46478 (13)	0.0154 (6)
C4	0.1727 (5)	0.52774 (16)	0.42608 (13)	0.0158 (6)
C5	-0.1008 (5)	0.50493 (18)	0.33862 (13)	0.0196 (6)
H5	-0.037379	0.452194	0.327658	0.024*
C4A	-0.0119 (4)	0.55400 (17)	0.38887 (13)	0.0161 (6)
C6	-0.2769 (5)	0.53228 (19)	0.30555 (15)	0.0237 (7)
H6	-0.332691	0.499128	0.271220	0.028*
C7	-0.3757 (5)	0.60896 (19)	0.32201 (15)	0.0241 (7)
H7	-0.504081	0.625506	0.300995	0.029*
C8	-0.2880 (5)	0.65997 (19)	0.36813 (14)	0.0209 (6)
H8	-0.352964	0.712802	0.377996	0.025*
C8A	-0.1007 (5)	0.63448 (17)	0.40134 (13)	0.0160 (6)
C31	0.4680 (4)	0.56876 (16)	0.50328 (13)	0.0158 (6)
C321	0.7023 (4)	0.61744 (16)	0.59179 (13)	0.0146 (6)
C322	0.6840 (5)	0.66241 (17)	0.64919 (14)	0.0173 (6)
H322	0.559581	0.695626	0.656408	0.021*
C323	0.8416 (4)	0.66032 (18)	0.69622 (14)	0.0184 (6)
C324	1.0277 (5)	0.61192 (18)	0.68531 (13)	0.0181 (6)
C325	1.0432 (5)	0.56727 (18)	0.62795 (14)	0.0191 (6)
H325	1.167921	0.534397	0.620254	0.023*
C326	0.8845 (4)	0.56865 (17)	0.58145 (14)	0.0168 (6)
H326	0.899709	0.536669	0.542929	0.020*
C327	0.8115 (5)	0.70814 (19)	0.75834 (15)	0.0250 (7)
H32A	0.934273	0.745612	0.765419	0.037*
H32B	0.800307	0.667948	0.794181	0.037*

H32C	0.680368	0.741992	0.755852	0.037*
C328	1.2038 (5)	0.6077 (2)	0.73465 (15)	0.0254 (7)
H32D	1.253251	0.665128	0.744633	0.038*
H32E	1.323221	0.574413	0.717458	0.038*
H32F	1.149786	0.580841	0.774012	0.038*
C411	0.1222 (5)	0.37148 (17)	0.41833 (14)	0.0194 (6)
C412	0.2064 (5)	0.30036 (17)	0.38929 (13)	0.0202 (7)
H412	0.346385	0.302560	0.371508	0.024*
C413	0.0886 (5)	0.22452 (18)	0.38552 (13)	0.0192 (6)
C414	-0.1149 (5)	0.22182 (18)	0.41275 (14)	0.0208 (7)
C415	-0.1955 (5)	0.29255 (18)	0.44308 (14)	0.0228 (7)
H415	-0.333552	0.290071	0.462158	0.027*
C416	-0.0793 (5)	0.36751 (18)	0.44637 (14)	0.0200 (6)
H416	-0.137324	0.415606	0.467629	0.024*
C417	0.1826 (5)	0.14893 (18)	0.35187 (16)	0.0275 (7)
H41D	0.090414	0.132683	0.315709	0.041*
H41E	0.193326	0.101625	0.382290	0.041*
H41F	0.325447	0.163163	0.335672	0.041*
C418	-0.2461 (5)	0.14148 (19)	0.40803 (16)	0.0281 (7)
H41A	-0.384750	0.150125	0.429087	0.042*
H41B	-0.169739	0.095098	0.429390	0.042*
H41C	-0.268722	0.127195	0.362554	0.042*

Atomic displacement parameters (Å²)

	U^{11}	U^{22}	U^{33}	U^{12}	U^{13}	U^{23}
O31	0.0180 (10)	0.0128 (9)	0.0356 (12)	0.0031 (8)	-0.0017 (9)	-0.0058 (9)
N1	0.0155 (12)	0.0137 (11)	0.0229 (13)	-0.0001 (10)	0.0022 (11)	-0.0008 (10)
N32	0.0136 (12)	0.0114 (11)	0.0236 (13)	0.0014 (10)	-0.0003 (10)	-0.0012 (10)
N41	0.0152 (13)	0.0120 (12)	0.0314 (14)	0.0002 (10)	-0.0025 (12)	-0.0058 (10)
C2	0.0173 (14)	0.0107 (13)	0.0202 (15)	-0.0031 (12)	0.0028 (12)	-0.0018 (11)
C3	0.0133 (14)	0.0137 (13)	0.0194 (14)	-0.0012 (12)	0.0052 (12)	-0.0011 (11)
C4	0.0152 (14)	0.0139 (13)	0.0184 (15)	-0.0010 (11)	0.0042 (12)	-0.0010 (11)
C5	0.0203 (15)	0.0159 (14)	0.0226 (15)	-0.0033 (13)	0.0013 (13)	-0.0032 (12)
C4A	0.0146 (14)	0.0146 (14)	0.0193 (14)	-0.0032 (12)	0.0040 (12)	0.0013 (11)
C6	0.0273 (17)	0.0212 (15)	0.0224 (15)	-0.0067 (14)	-0.0068 (14)	-0.0013 (12)
C7	0.0203 (16)	0.0232 (16)	0.0287 (17)	-0.0014 (13)	-0.0065 (13)	0.0028 (13)
C8	0.0195 (15)	0.0171 (14)	0.0260 (16)	0.0008 (13)	0.0010 (13)	0.0024 (12)
C8A	0.0164 (14)	0.0138 (13)	0.0179 (14)	-0.0031 (12)	0.0048 (12)	-0.0003 (11)
C31	0.0145 (14)	0.0123 (12)	0.0208 (15)	-0.0020 (12)	0.0057 (12)	0.0000 (12)
C321	0.0136 (14)	0.0103 (13)	0.0200 (14)	-0.0020 (11)	0.0009 (12)	0.0035 (11)
C322	0.0163 (14)	0.0118 (13)	0.0238 (16)	-0.0002 (12)	0.0036 (12)	0.0004 (11)
C323	0.0171 (14)	0.0180 (14)	0.0202 (15)	-0.0030 (13)	0.0036 (12)	0.0041 (11)
C324	0.0159 (15)	0.0152 (14)	0.0232 (15)	-0.0035 (12)	0.0031 (12)	0.0057 (12)
C325	0.0138 (14)	0.0168 (14)	0.0267 (16)	0.0018 (12)	0.0048 (12)	0.0032 (12)
C326	0.0151 (14)	0.0148 (13)	0.0205 (15)	-0.0018 (11)	0.0034 (12)	-0.0011 (12)
C327	0.0246 (16)	0.0234 (16)	0.0269 (17)	0.0001 (14)	0.0022 (14)	-0.0033 (13)
C328	0.0186 (16)	0.0316 (17)	0.0261 (16)	-0.0015 (14)	0.0003 (13)	0.0025 (13)

C411	0.0241 (16)	0.0132 (13)	0.0208 (15)	-0.0013 (12)	-0.0066 (13)	-0.0002 (12)
C412	0.0225 (16)	0.0174 (14)	0.0209 (16)	0.0005 (13)	-0.0013 (13)	0.0001 (12)
C413	0.0279 (17)	0.0128 (14)	0.0171 (15)	0.0022 (12)	-0.0057 (13)	-0.0007 (11)
C414	0.0223 (16)	0.0205 (15)	0.0197 (16)	-0.0021 (12)	-0.0065 (13)	0.0028 (12)
C415	0.0198 (15)	0.0252 (16)	0.0235 (16)	-0.0019 (13)	-0.0022 (13)	0.0035 (12)
C416	0.0206 (15)	0.0150 (14)	0.0245 (16)	0.0005 (12)	-0.0025 (13)	-0.0018 (12)
C417	0.0307 (17)	0.0171 (15)	0.0347 (18)	-0.0001 (14)	0.0016 (15)	-0.0046 (13)
C418	0.0298 (18)	0.0213 (16)	0.0333 (18)	-0.0062 (14)	-0.0042 (15)	0.0036 (13)

Geometric parameters (Å, °)

O31—C31	1.238 (3)	C323—C327	1.505 (4)
N1—C2	1.315 (4)	C324—C325	1.386 (4)
N1—C8A	1.367 (4)	C324—C328	1.505 (4)
N32—C31	1.350 (3)	C325—C326	1.384 (4)
N32—C321	1.416 (4)	C325—H325	0.9500
N32—H32	0.90 (4)	C326—H326	0.9500
N41—C4	1.364 (3)	C327—H32A	0.9800
N41—C411	1.437 (4)	C327—H32B	0.9800
N41—H41	0.84 (4)	C327—H32C	0.9800
C2—C3	1.416 (4)	C328—H32D	0.9800
C2—H2	0.96 (3)	C328—H32E	0.9800
C3—C4	1.405 (4)	C328—H32F	0.9800
C3—C31	1.494 (4)	C411—C412	1.379 (4)
C4—C4A	1.449 (4)	C411—C416	1.389 (4)
C5—C6	1.367 (4)	C412—C413	1.408 (4)
C5—C4A	1.413 (4)	C412—H412	0.9500
C5—H5	0.9500	C413—C414	1.392 (4)
C4A—C8A	1.411 (4)	C413—C417	1.503 (4)
C6—C7	1.401 (4)	C414—C415	1.377 (4)
C6—H6	0.9500	C414—C418	1.514 (4)
C7—C8	1.365 (4)	C415—C416	1.390 (4)
C7—H7	0.9500	C415—H415	0.9500
C8—C8A	1.417 (4)	C416—H416	0.9500
C8—H8	0.9500	C417—H41D	0.9800
C321—C322	1.391 (4)	C417—H41E	0.9800
C321—C326	1.391 (4)	C417—H41F	0.9800
C322—C323	1.387 (4)	C418—H41A	0.9800
C322—H322	0.9500	C418—H41B	0.9800
C323—C324	1.410 (4)	C418—H41C	0.9800
C2—N1—C8A	117.2 (2)	C326—C325—C324	122.7 (3)
C31—N32—C321	126.6 (2)	C326—C325—H325	118.7
C31—N32—H32	119 (2)	C324—C325—H325	118.7
C321—N32—H32	114 (2)	C325—C326—C321	119.2 (3)
C4—N41—C411	125.7 (2)	C325—C326—H326	120.4
C4—N41—H41	112 (2)	C321—C326—H326	120.4
C411—N41—H41	115 (2)	C323—C327—H32A	109.5

N1—C2—C3	125.9 (3)	C323—C327—H32B	109.5
N1—C2—H2	111.9 (17)	H32A—C327—H32B	109.5
C3—C2—H2	122.2 (17)	C323—C327—H32C	109.5
C4—C3—C2	117.6 (3)	H32A—C327—H32C	109.5
C4—C3—C31	121.3 (2)	H32B—C327—H32C	109.5
C2—C3—C31	120.9 (2)	C324—C328—H32D	109.5
N41—C4—C3	121.9 (3)	C324—C328—H32E	109.5
N41—C4—C4A	120.6 (2)	H32D—C328—H32E	109.5
C3—C4—C4A	117.4 (2)	C324—C328—H32F	109.5
C6—C5—C4A	120.9 (3)	H32D—C328—H32F	109.5
C6—C5—H5	119.5	H32E—C328—H32F	109.5
C4A—C5—H5	119.5	C412—C411—C416	119.5 (3)
C8A—C4A—C5	118.3 (3)	C412—C411—N41	119.0 (3)
C8A—C4A—C4	118.3 (2)	C416—C411—N41	121.5 (2)
C5—C4A—C4	123.3 (3)	C411—C412—C413	121.2 (3)
C5—C6—C7	120.4 (3)	C411—C412—H412	119.4
C5—C6—H6	119.8	C413—C412—H412	119.4
C7—C6—H6	119.8	C414—C413—C412	118.8 (3)
C8—C7—C6	120.3 (3)	C414—C413—C417	121.4 (3)
C8—C7—H7	119.9	C412—C413—C417	119.8 (3)
C6—C7—H7	119.9	C415—C414—C413	119.6 (3)
C7—C8—C8A	120.3 (3)	C415—C414—C418	120.7 (3)
C7—C8—H8	119.9	C413—C414—C418	119.6 (3)
C8A—C8—H8	119.9	C414—C415—C416	121.5 (3)
N1—C8A—C4A	122.8 (3)	C414—C415—H415	119.3
N1—C8A—C8	117.7 (3)	C416—C415—H415	119.3
C4A—C8A—C8	119.5 (3)	C411—C416—C415	119.4 (3)
O31—C31—N32	121.4 (3)	C411—C416—H416	120.3
O31—C31—C3	121.1 (2)	C415—C416—H416	120.3
N32—C31—C3	117.4 (2)	C413—C417—H41D	109.5
C322—C321—C326	118.8 (3)	C413—C417—H41E	109.5
C322—C321—N32	116.8 (2)	H41D—C417—H41E	109.5
C326—C321—N32	124.3 (2)	C413—C417—H41F	109.5
C323—C322—C321	122.1 (3)	H41D—C417—H41F	109.5
C323—C322—H322	119.0	H41E—C417—H41F	109.5
C321—C322—H322	119.0	C414—C418—H41A	109.5
C322—C323—C324	119.1 (3)	C414—C418—H41B	109.5
C322—C323—C327	120.1 (3)	H41A—C418—H41B	109.5
C324—C323—C327	120.8 (3)	C414—C418—H41C	109.5
C325—C324—C323	118.1 (3)	H41A—C418—H41C	109.5
C325—C324—C328	120.7 (3)	H41B—C418—H41C	109.5
C323—C324—C328	121.2 (3)		
C8A—N1—C2—C3	-5.5 (4)	C2—C3—C31—N32	5.0 (4)
N1—C2—C3—C4	1.1 (4)	C31—N32—C321—C322	-150.3 (3)
N1—C2—C3—C31	-174.0 (3)	C31—N32—C321—C326	31.7 (4)
C411—N41—C4—C3	141.0 (3)	C326—C321—C322—C323	0.2 (4)
C411—N41—C4—C4A	-41.6 (4)	N32—C321—C322—C323	-177.9 (2)

C2—C3—C4—N41	-175.7 (3)	C321—C322—C323—C324	0.8 (4)
C31—C3—C4—N41	-0.6 (4)	C321—C322—C323—C327	-178.3 (3)
C2—C3—C4—C4A	6.8 (4)	C322—C323—C324—C325	-0.9 (4)
C31—C3—C4—C4A	-178.1 (2)	C327—C323—C324—C325	178.1 (3)
C6—C5—C4A—C8A	-4.1 (4)	C322—C323—C324—C328	179.8 (3)
C6—C5—C4A—C4	179.2 (3)	C327—C323—C324—C328	-1.2 (4)
N41—C4—C4A—C8A	172.4 (3)	C323—C324—C325—C326	0.1 (4)
C3—C4—C4A—C8A	-10.1 (4)	C328—C324—C325—C326	179.4 (3)
N41—C4—C4A—C5	-10.8 (4)	C324—C325—C326—C321	0.8 (4)
C3—C4—C4A—C5	166.7 (3)	C322—C321—C326—C325	-1.0 (4)
C4A—C5—C6—C7	-1.5 (4)	N32—C321—C326—C325	176.9 (2)
C5—C6—C7—C8	4.7 (5)	C4—N41—C411—C412	155.0 (3)
C6—C7—C8—C8A	-2.2 (4)	C4—N41—C411—C416	-27.8 (4)
C2—N1—C8A—C4A	1.7 (4)	C416—C411—C412—C413	2.3 (4)
C2—N1—C8A—C8	-175.7 (2)	N41—C411—C412—C413	179.6 (3)
C5—C4A—C8A—N1	-170.9 (3)	C411—C412—C413—C414	-1.1 (4)
C4—C4A—C8A—N1	6.0 (4)	C411—C412—C413—C417	178.3 (3)
C5—C4A—C8A—C8	6.4 (4)	C412—C413—C414—C415	-0.5 (4)
C4—C4A—C8A—C8	-176.7 (2)	C417—C413—C414—C415	-179.9 (3)
C7—C8—C8A—N1	174.1 (3)	C412—C413—C414—C418	178.7 (3)
C7—C8—C8A—C4A	-3.4 (4)	C417—C413—C414—C418	-0.6 (4)
C321—N32—C31—O31	-3.1 (4)	C413—C414—C415—C416	1.0 (4)
C321—N32—C31—C3	173.8 (2)	C418—C414—C415—C416	-178.3 (3)
C4—C3—C31—O31	6.9 (4)	C412—C411—C416—C415	-1.8 (4)
C2—C3—C31—O31	-178.1 (3)	N41—C411—C416—C415	-179.1 (3)
C4—C3—C31—N32	-170.0 (3)	C414—C415—C416—C411	0.2 (4)

Hydrogen-bond geometry (Å, °)

Cg is the centroid of the N1/C2—C4/C4A/C8A ring.

<i>D</i> —H... <i>A</i>	<i>D</i> —H	H... <i>A</i>	<i>D</i> ... <i>A</i>	<i>D</i> —H... <i>A</i>
N41—H41...O31	0.84 (4)	1.93 (3)	2.635 (3)	142 (3)
C326—H326...O31	0.95	2.40	2.887 (3)	112
N32—H32...N1 ⁱ	0.90 (4)	2.07 (4)	2.891 (3)	150 (3)
C2—H2...N1 ⁱ	0.96 (3)	2.55 (3)	3.477 (4)	163 (2)
C416—H416...O31 ⁱⁱ	0.95	2.39	3.252 (4)	150
C326—H326...Cg ⁱⁱⁱ	0.95	2.82	3.398 (3)	120

Symmetry codes: (i) $x+1/2, -y+3/2, -z+1$; (ii) $x-1, y, z$; (iii) $x+1, y, z$.